

White Paper

EXNERO

SEKA

Contents

1. Core Concepts and Design Approach 04

1.1 Design Objective Analysis 04

1.2 Multi-Factor Balance 05

1.3 Aerodynamic–Weight Crossover Analysis 06

1.4 Design Objectives and Optimization Strategy 10

2. Aerodynamics 12

2.1 Frontal Projected Area 12

2.2 Tube Profile Optimization 13

2.3 Aerodynamic Optimization of the MAG Bottle System 15

2.4 Wind-Tunnel Testing 19

2.4.1 Three-Stage Wind-Tunnel Test Program 19

2.4.2 Wind-Tunnel Test Conditions and Methodology 20

2.4.3 Wind-Tunnel Test Results 22

3 Torsional Stiffness 29

4 System Weight 30

5 Geometry 31

References 33

Glossary A 34

Appendix A Cycling Power Calculation Equations 35

Appendix B Aerodynamic–Weight Crossover Analysis 36

Appendix C Data Scope and Limitations 40

1

Design Approach & Core Concepts

$$P_{\text{total}} = P_{\text{Aer}}$$

$$P = \frac{1}{2}\rho C_d A\left(\frac{v}{3.6}\right)^3 + gm\left(C_{rr} + \frac{G}{100}\right)\left(\frac{v}{3.6}\right)$$

Core Concepts and Thinking

1.1 Design Objective Analysis

Road racing is not won by chasing the best numbers in a wind tunnel.

A road race is never a steady-state scenario. Riders are constantly moving between flat-road cruising, climbing, attacks and sprints, descending and high-speed cornering, and sustained efforts late in the race. Each scenario places different demands on speed retention, acceleration, power transfer efficiency, handling stability and rider fatigue.

A race bike therefore cannot be defined by a single performance parameter pushed to the extreme.

Aerodynamics, weight, overall torsional stiffness, geometry and handling response, and vertical compliance all need to work together as a system.

ExAero was developed around this principle: to bring these often competing parameters into balance, so the bike can deliver the performance that matters most in each racing scenario.

The goal is greater efficiency, more immediate response and consistent, predictable performance as the demands of the race continue to change.

Race Scenarios	Key Performance Demands	Performance Parameters
· Flat-road cruising · Climbing · Attacks and sprints · Descending and high-speed cornering · Sustained performance late in the race	· Speed retention · Acceleration · Power transfer efficiency · Handling stability · Reduced rider fatigue	· CdA · Weight · Overall torsional stiffness · Handling response · Vertical compliance · Geometry

A race is never a single, steady-state scenario. The demands are constantly shifting, and the performance priorities change with them. ExAero is designed to balance these competing parameters as an integrated system, rather than optimizing each one in isolation.

1.2 Multi-Factor Balance

Reducing local tube cross-sections can lower projected frontal area, but it may also make those sections less aerodynamically efficient at certain yaw angles. It will also often reduce the frame's overall torsional stiffness, which may require additional material in key areas to recover the required stiffness.

For this reason, minimizing tube sections does not necessarily result in a lighter bike, nor does it necessarily improve overall system performance.

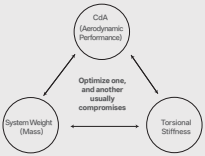

Rather than minimizing frontal area (A), the aim is to keep it within an effective range. Aerodynamic performance is then improved through shape optimization that reduces the drag coefficient (Cd). At the same time, the design must retain sufficient torsional stiffness without adding unnecessary volume.

Structural performance depends not only on the material itself, but also on how loads are carried, how efficiently each section is shaped, and how the material is distributed. This allows aerodynamics, weight, and overall stiffness to be balanced as part of the same design.

1.3 Aerodynamic–Weight Crossover Analysis

Martin JC, Douglas ML, Cobb JE, McFadden KL and Coggan AR decomposed road cycling power into several physical components:

$$\cdot P_{\text{Athlete}} = P_{\text{NET}} = P_{\text{Aero}} + P_{\text{RR}} + P_{\text{WB}} + P_{\text{PE}} + P_{\text{KE}}$$

where P_{Aero} represents aerodynamic power, P_{RR} rolling resistance power, P_{WB} wheel-bearing resistance power, P_{PE} potential energy power associated with climbing, and P_{KE} kinetic energy power associated with acceleration.

When drivetrain efficiency η, wheel-bearing resistance P_{WB}, and acceleration-related power P_{KE} are temporarily excluded, and the analysis is limited to relatively steady-state road riding, the model can be simplified to the three dominant components: aerodynamic power, rolling resistance power, and climbing power.

$$P_{\text{total}} = P_{\text{Aero}} + P_{\text{RR}} + P_{\text{PE}}$$

Expanding these terms gives:

$$P = \frac{1}{2}\rho C_d A\left(\frac{v}{3.6}\right)^3 + gm\left(C_{rr} + \frac{G}{100}\right)\left(\frac{v}{3.6}\right)$$

Where:

ρ	CdA	m	Crr	$G\%$	g
Air density	Drag area	Mass	Coefficient of rolling resistance	Gradient	Gravitational acceleration

Based on the simplified model above, we consider the following question:

Under different riding conditions, which provides the greater benefit: a 3 W aerodynamic power saving or a 120 g reduction in system mass?*

*The 3 W aerodynamic saving is defined at 45 km/h.

Assuming an aerodynamic power saving of 3 W at 45 km/h, the equivalent saving at other speeds is:

$$\Delta P_{\text{Aero}}(v) = 3\left(\frac{v}{45}\right)^3$$

For the full calculation method, see Appendix B.

The power saving associated with a 120 g reduction in system mass is:

$$\Delta P_{\text{Mass}} = g \cdot \Delta m \cdot \left(C_{rr} + \frac{G}{100}\right) \cdot \left(\frac{v}{3.6}\right)$$

$$\Delta m = 0.12\,\text{kg}$$

The crossover point occurs when the aerodynamic power saving equals the power saving from the mass reduction:

$$\Delta P_{\text{Aero}}(v) = \Delta P_{\text{Mass}}$$

Aerodynamic saving at the current speed

Power saving from a 120 g mass reduction at the current gradient

Expanding the equation:

$$3\left(\frac{v}{45}\right)^3 = g \cdot 0.12 \cdot \left(C_{rr} + \frac{G}{100}\right) \cdot \left(\frac{v}{3.6}\right)$$

Based on this model, the gradient and speed at which the aerodynamic power saving equals the power saving associated with the mass reduction can be determined.
(Aerodynamic-Weight Crossover Point)

Assumptions used in the calculation

- $\rho = 1.20\,\mathrm{kg/m^3}$
- $C_dA = 0.3398$

  Measured for the ExAero RDC with two ExAero MAG bottles at 45 km/h in the wind tunnel, including the rider.
- $m = 85\,\mathrm{kg}$

  Total bike–rider system mass, including bottles, water and rider equipment.
- $C_{rr} = 0.003$

  A representative rolling-resistance value for a high-performance road bike on good paved roads.

Using different rider power outputs gives the following results:

Rider Power	Crossover Gradient	Crossover Speed
150 W	4.1%	20.8 km/h
100 W	4.8%	22.1 km/h
150 W	5.2%	23.3 km/h
200 W	5.7%	24.4 km/h
250 W	6.2%	25.3 km/h

Assumptions: steady speed, constant rider power, no acceleration, and unchanged riding position. Tire deformation, drivetrain efficiency, changes in wind direction, and variations in rider pacing are not considered.

Calculating the results across different rider power outputs and average gradients gives:

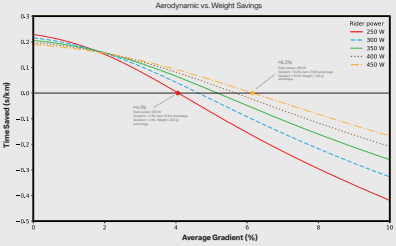

Aerodynamic–Weight Crossover Analysis

Taking a 250 W rider as an example, the aerodynamic and weight benefits reach the crossover point at an average gradient of approximately 4.1%.

Below this gradient, the aerodynamic advantage is greater; above it, the benefit of lower weight gradually becomes greater.

As rider power and riding speed increase, the crossover point between aerodynamic and weight benefits shifts toward steeper gradients.

At higher speeds, aerodynamic drag accounts for a greater share of the total resistance, increasing the relative benefit of aerodynamic improvements.

1.4 Design Objectives and Optimization Strategy

Based on the analysis of key performance parameters, the trade-offs between them, and the aerodynamic–weight crossover model, ExAero was approached as a multi-objective optimization problem, rather than an attempt to maximize any single performance metric.

For ExAero, frontal area A is allowed to vary within a controlled range. This provides more room for structural design, improves section efficiency, and allows a better balance between stiffness and weight. At the same time, tube shapes and overall system integration are optimized to reduce system CdA and improve aerodynamic efficiency.

From a structural perspective, geometry and structural design are used to increase torsional stiffness, while weight is allowed to vary within defined limits to improve power transfer and handling response. Vertical compliance is maintained at the target level to help reduce rider fatigue.

Final objective:

To establish a system-level balance between aerodynamic efficiency, structural performance, and ride characteristics, improving overall performance rather than optimizing any single parameter in isolation.

Optimization Variable	Design Direction
Frontal Area	Controlled increase
System CdA	More than 3 W reduction at 45 km/h
Overall Torsional Stiffness	Improve structural stiffness and power transfer
Weight	Controlled within design constraints
Vertical compliance	Maintain target level

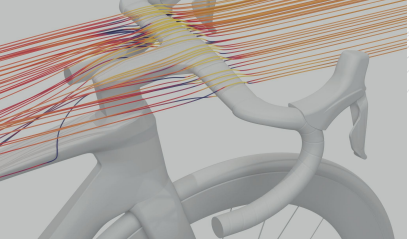

2

AERODYNAMICS

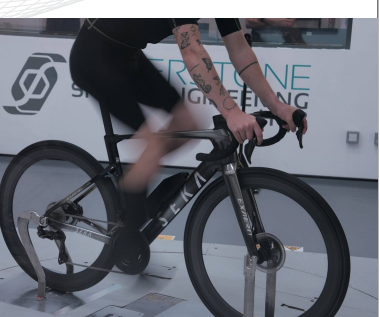

2.1 Frontal Projected Area

Spear already achieved good aerodynamic efficiency with a relatively small frontal projected area. For ExAero, the objective was not to further minimize local projected area, but to allow controlled changes in frontal area at the system level.

This provided more room to optimize tube cross-sections, structural stiffness, and overall frame design. A larger frontal area does not necessarily result in higher system drag. Through tube-shape optimization and component integration, the overall objective remained to reduce system CdA.

The chart below compares the frontal projected areas of the key components on ExAero and Spear, showing how the frame, fork, and handlebar have changed in terms of projected area.

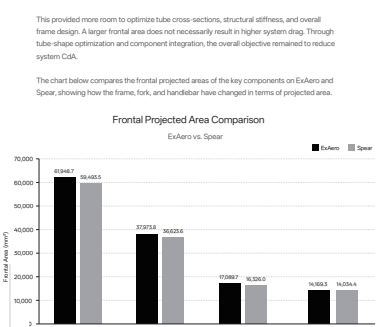

Total System Δ	Key Drivers of Increase
+ 2,455.2 mm² (+4.13%)	• Frame: +1,350.2 mm² (+3.69%) • Fork including 185 mm steering tube: +763.7 mm² (+4.68%) • Handlebar: +134.9 mm² (+0.96%)

Compared with Spear, ExAero has a 2,455.2 mm² increase in total frontal projected area, equivalent to 4.13%. Most of this increase comes from the frame and fork.

2.2 Tube Profile Optimization

The front triangle is a key structural and aerodynamic region of the frame. Its geometry directly affects frontal area, form drag, and structural stiffness. Rather than applying a uniform scaling to the tube profiles, ExAero uses targeted changes to the head tube, down tube, and fork junction according to the aerodynamic and structural requirements of each area.



Figure 2.2.1
Side View Projection, Proto A vs. ExAero

ExAero treats the front triangle as a primary area for optimization, with the aim of balancing aerodynamic efficiency and structural performance.

Compared with Spear, both Proto A and ExAero have a larger frontal projected area. With section width held constant, tube depth was increased to evaluate how changes in profile geometry affect aerodynamic performance.

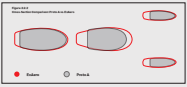

Figure 2.2.3
CFD Flow Field Comparison:

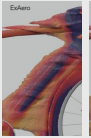

The wake remains more concentrated, with a smaller region of local disturbance and improved flow continuity.

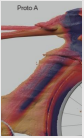

The wake is more dispersed, with a larger region of local disturbance and less continuous downstream flow.

The CFD comparison shows the flow around Proto A and ExAero, the final prototype, under the same boundary conditions. The analysis focuses on wake width, flow attachment, and local flow structures to assess how the geometric changes influence the resulting flow field.

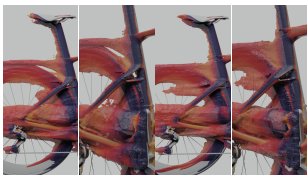

ExAero Proto A

Under the same visualization settings, ExAero shows a more concentrated wake in the interaction region between the seat tube and rear wheel, with a smaller area of strong local disturbance. This flow-field trend is consistent with the calculated system drag.

CFD Analysis

ExAero and Proto A were evaluated using CFD under the same boundary conditions. The simulation speed was set to 45 km/h, with yaw angles of 1°, 6°, and 15° assessed separately.

	ExAero RDC			Proto A		
Test Configuration	45 km/h, standard handlebar (~20 mm stack), no bottles, Zipp 101s wheelset with P Zero Race 28 tires, simplified wheelset			45 km/h, standard handlebar (~20 mm stack), no bottles, Zipp 101s wheelset with P Zero Race 28 tires, simplified wheelset		
Yaw Angle (°)	1°	6°	15°	1°	6°	15°
Yaw Angle (rad)	0.0175	0.1047	0.2618	0.0175	0.1047	0.2618
Case	ExAero 1°	ExAero 6°	ExAero 15°	Proto A 1°	Proto A 6°	Proto A 15°
Standard Deviation (S.D.)	0	0	0	0.0001	0.0001	0.0002
Frame Drag (N)	1.3765	1.4623	1.5333	1.4437	1.5286	1.5811
Fork Drag (N)	0.4423	0.3641	0.2346	0.4818	0.4075	0.4188
Handlebar Drag (N)	0.6818	0.6673	0.7297	0.6351	0.6616	0.7310
Total System Drag (N)	0.5406	0.5704	0.5988	0.5648	0.6007	0.5701
CdA (m²)	0.0467	0.0488	0.0537	0.0497	0.0481	0.0544
Aerodynamic Power (W)	56.67	56.69	62.75	58.06	56.20	63.68

The CFD results below compare the system-level aerodynamic performance at different yaw angles at 45 km/h.

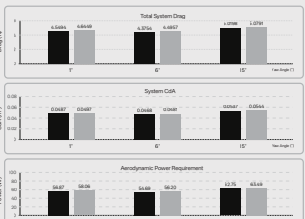

The CFD results show lower total system drag for ExAero at each yaw angle tested, corresponding to approximately 0.74–1.51 W of aerodynamic power saving at 45 km/h. The changes to the tube profiles and junction areas reduce system drag across the tested yaw range.

2.3 Aerodynamic Optimization of the MAG Bottle System

Bottle shape and mounting position affect the local flow around the down tube, seat tube, and surrounding frame surfaces. For this reason, the bottle system was developed as part of the bike's overall aerodynamic system rather than as an isolated component. The study considered bottle shape, mounting position, and the interaction between the bottles and adjacent frame tube profiles.

Building on the existing test results, CFD analysis was used to further isolate individual variables and evaluate the flow interaction between the MAG aero bottle system and the ExAero frame.



Working with AeroCoach, we carried out CFD analysis of the MAG bottle system to evaluate how bottle shape, mounting position, and its interaction with the frame tube profiles affect overall system drag. The results were used to guide further design development.

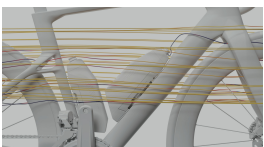

Figure 2.3.1

CFD streamline visualization around the down tube and bottle area, showing the interaction of the front-wheel wake with the bottles and surrounding frame surfaces.



The aerodynamic performance of the bottle system depends on the combined effect of bottle shape, mounting position, and the surrounding frame geometry. As the front-wheel wake passes through this region, these factors together influence the local flow path and the extent of flow disturbance.

Figure 2.3.2

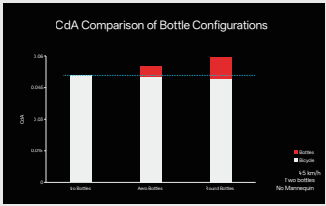

After the bottles are installed, the CdA contribution from the bicycle itself decreases in both configurations, indicating that the bottles alter the flow around the front-wheel wake and down tube. The reduction is greater with the round bottles. However, the round bottles themselves have substantially higher CdA than the MAG aero bottles, resulting in the highest total system CdA.

Conclusion

The CFD results show that a bottle should not be evaluated as an isolated component. Its shape affects the front-wheel wake and the flow around the down tube and adjacent frame surfaces. However, the final aerodynamic performance depends on the combined drag of the bicycle and the bottles.

Compared with round bottles, the MAG system maintains a similar influence on the surrounding flow while substantially reducing the drag of the bottles themselves.

Converted to Power

Comparison	ΔCdA	Power Difference
ExAero MAG vs. No Bottles	+0.0043	+5.04 W
Round Bottles vs. No Bottles	+0.0085	+9.96 W
Round Bottles vs. ExAero MAG	+0.0042	+4.92 W

Wind tunnel tests



2.4 Wind-Tunnel Testing

2.4.1 Three-Stage Wind-Tunnel Test Program

The wind-tunnel program was divided into three stages to isolate key variables and provide consistent comparisons. For tests conducted on different dates, the Spear was used as one of the test objects and also as the reference in each test.



Stage 1 — Baseline Comparison

Proto A, the baseline ExAero configuration (without the MAG bottle system or Gradient ALTA cockpit), and benchmark bikes were tested.

This stage is used to verify the consistency between CFD predictions and wind tunnel results, and to establish the baseline reference required for subsequent testing.

Stage 2 — Complete Aero System

The MAG bottle system was added to evaluate the aerodynamic effect of bottle shape, position, and interaction with the ExAero frame.

Results were compared with the Spear baseline.

Stage 3 — Extended Configuration

The Gladius ALTA cockpit and a one-size-smaller frame were added while maintaining the same target rider position and contact points.

This stage evaluated how frame size and cockpit configuration affect overall aerodynamic performance.

2.4.2 Wind-Tunnel Test Conditions and Methodology

Wind-tunnel testing was conducted by AeroCoach at the Silverstone Sports Engineering Hub (SSEH). The facility is specifically designed for aerodynamic testing of bicycle–rider systems, allowing dynamic yaw sweeps and full-system drag measurements.

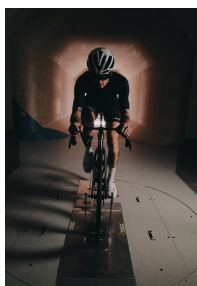

Test Conditions
The wind-tunnel tests were conducted under controlled conditions:
Air density: 1.2 kg/m³
Effective airspeed: 45 km/h

Performance Calculation Assumptions
Road gradient: 0%
Coefficient of rolling resistance: 0.0045

Yaw-Weighting Method
The measured CdA–yaw data were weighted using the yaw-angle probability distribution proposed by Barry, N. (2018), giving a weighted mean CdA for whole-bike comparison.

Rider Simulation
Depending on the test objective, either a static dummy-leg setup or a real rider pedaling dynamically was used. Results are compared only between configurations tested with the same rider-simulation method.



Data Acquisition
Tests used a continuous yaw sweep from -20° to +20°. The bicycle was rotated at 0.167°/s, with aerodynamic data sampled continuously at 0.01-second intervals. Each configuration was tested over multiple repeat runs to quantify the aerodynamic contribution of individual components and the complete system.

Data Processing

Approximately 280,000 raw data points were collected for each test configuration. After the dynamic yaw sweep, the data were grouped into predefined yaw-angle ranges and statistically processed. Mean CdA values at representative yaw angles were then weighted using the method proposed by Barry, N. (2018), producing a weighted mean CdA for comparison between configurations.

Bicycle Setup and Test Details

The tests were conducted with key variables held constant:

· Wheels: Zipp 404 Firecrest, unchanged across all tests.
· Tires: Pirelli P Zero 28C tubeless, unchanged across all tests.
· Groupset: Shimano Dura-Ace R9270 Di2, unchanged across all tests.
· Bottle cages: Tacx Deva ×2, unchanged throughout Stage 1.
· Bottles: 74 mm diameter, 590 ml ×2, unchanged across all tests.
· The ExAero MAG bottles used in testing were development prototypes and differ slightly in shape from the final production version.
· The Spear aero bottle cage already provides some aerodynamic benefit compared with a conventional round-bottle setup.

Bicycle Setup and Rider Position Matching

To make the comparison between platforms as consistent as possible, frame size, front-end setup, and rider contact points were matched as closely as practical.

ExAero and Proto A in size 54 both use a frame geometry of 542 mm stack and 383 mm reach. The 2025 Canyon Aeroad CFR in size S has a stack of 539 mm and a reach of 390 mm. ExAero and Proto A were fitted with integrated handlebars ranging from 375 to 420 mm in width, while the Aeroad adjustable cockpit was set to 400 mm.

To account for differences in stack, reach, and cockpit design between bikes, spacer height and brake-hood position were adjusted during testing to keep rider contact points and riding position as consistent as possible. This reduced the influence of geometric differences on the aerodynamic results.

All dimensional measurements, position adjustments, and test setups were carried out by AeroCoach using the same standards throughout the test program.

2.4.3 Wind-Tunnel Test Results

Stage 1 — Baseline System Comparison

Proto A Size 54	ExAero RDC Size 54	Canyon Aeroad CFR 2025 Size S
Tacx Deva 74 mm bottle ×2	Tacx Deva 74 mm bottle ×2	Tacx Deva 74 mm bottle ×2







Test Results (Rider on the Hoods)

Yaw angle	Weighting function (Barry 2018)	ExAero RDC Round bottles ×2	Proto A Round bottles ×2	Canyon Round bottles ×2
20	0.09	0.033593176	0.034181781	0.03307499
-17.5	0.158	0.056519234	0.058237236	0.056773624
-15	0.237	0.086852368	0.089277941	0.084449638
-12.5	0.277	0.135588758	0.133462779	0.134292566
-10	0.543	0.189805471	0.187704782	0.188792688
-7.5	0.683	0.233343851	0.23171474	0.232461928
-5	0.857	0.292094048	0.29043808	0.296585995
-2.5	0.952	0.329992359	0.329810363	0.333216189
0	1	0.341164281	0.342315236	0.348960668
2.5	0.952	0.329061657	0.326801913	0.331987501
5	0.857	0.295215273	0.292239881	0.296014779
7.5	0.683	0.23207302	0.230444626	0.234566642
10	0.543	0.186488645	0.189955143	0.18829879
12.5	0.277	0.13474423	0.132465467	0.13542079
15	0.237	0.082541725	0.083503253	0.082638036
17.5	0.158	0.055389165	0.055872542	0.054668006
20	0.09	0.032396055	0.032215066	0.031500141
Weighting	**0.794**	**0.343726393**	**0.344288511**	**0.347372131**

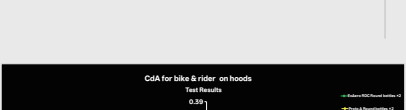

Stage 1 showed that the performance trend predicted by CFD during development was broadly consistent with the wind-tunnel results. Although the absolute values differed, CFD correctly identified the direction of improvement and provided a useful basis for further design development.

Compared with Proto A, ExAero reduced weighted CdA by 0.00056 m^2, equivalent to approximately 0.66 W of aerodynamic power saving at 45 km/h.

Compared with the Canyon Aeroad CFR 2025 benchmark, ExAero achieved a 0.00165 m^2 lower weighted CdA, equivalent to approximately 1.93 W of aerodynamic power saving at 45 km/h.

The results show that ExAero further reduced drag relative to Proto A and, under these test conditions, also outperformed the selected benchmark bike.

Stage 2 — Complete Aero System

ExAero RDC Size S4	ExAero RDC Size S4	Spear RDC Size M
MAG aero bottle	MAG aero bottle only downtube	aero bottle cage 74 mm bottle *2



Test Results (Rider on the Hoods)

Yaw angle	Weighting function (Barry 2016)	ExAero RDC Aero bottles *2	ExAero RDC Aero bottle downtube	Spear Round bottles *2
-20	0.09	0.032163099	0.032364007	0.034237970
-17.5	0.158	0.057223437	0.056771909	0.058619527
-15	0.257	0.095818201	0.094631496	0.098502743
-12.5	0.377	0.132759583	0.132014698	0.138139327
-10	0.543	0.187758829	0.186481512	0.192822961
-7.5	0.683	0.231283781	0.229470869	0.239288213
-5	0.837	0.286512223	0.283447658	0.287386481
-2.5	0.932	0.315969986	0.31987738	0.319729371
0	1	0.339087303	0.339479974	0.338429932
2.5	0.932	0.320734297	0.32019485	0.322279748
5	0.837	0.289933509	0.290587697	0.29186537
7.5	0.683	0.2500212	0.2516075468	0.250857764
10	0.543	0.18389603	0.183359798	0.183534121
12.5	0.377	0.129773287	0.129095585	0.129163321
15	0.257	0.0826283	0.08136837	0.082256635
17.5	0.158	0.050389429	0.0502921703	0.050150131
20	0.09	0.032140837	0.0321521378	0.032158466
Weighting	**6.79%**	**0.339383267**	**0.338327182**	**0.342977761**

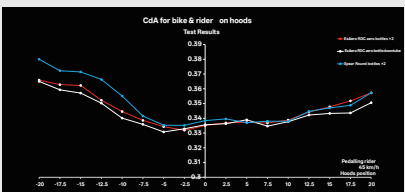

Stage 2 focused on the performance of the complete ExAero aerodynamic system, comparing it with the complete Spear system and evaluating the difference between single- and dual-MAG bottle configurations.

Compared with the Spear RDC fitted with its original aero bottle cages and two 74 mm round bottles, the ExAero RDC with two MAG aero bottles reduced weighted CdA by 0.00314 m^2, equivalent to approximately 3.68 W of aerodynamic power saving at 45 km/h.

The test also showed that the configuration with a single MAG aero bottle on the down tube had an even lower weighted CdA. Compared with the single-bottle setup, the dual-bottle setup increased weighted CdA by 0.00151 m^2, corresponding to approximately 1.77 W of additional power at 45 km/h.

It should be noted that the Spear baseline used its original aero bottle cages rather than conventional external bottle cages, giving it an inherent aerodynamic advantage.

Under these test conditions, the complete ExAero system saved approximately 3.68 W at 45 km/h compared with the complete Spear system. The single-down-tube MAG bottle configuration provided a further 1.77 W aerodynamic advantage.

Stage 3 — Extended Configuration

ExAero RDC Size S2	ExAero RDC Size S2	Spear RDC Size M
Gladius ALTA handlebar MAG aero bottle	Gladius ALTA handlebar MAG aero bottle only downtube	Aero bottle cage 74 mm bottle +2

Stage 3 explored the aerodynamic effect of using a one-size-smaller ExAero frame with the Gladius ALTA cockpit while maintaining the same rider position and contact points.

Test Results — Rider on the Hoods

Yaw angle	Weighting function (Barry 2018)	Spear 2 round bottles w rider	ExAero 2 aero bottles w rider	ExAero 1 aero bottle downtube w rider
-20	0.09	3.658833382	3.658833384	0.0379475
-17.5	0.138	3.097361583	3.098818874	0.0868787482
-15	0.237	3.100208994	3.09700872	0.0868777188
-12.5	0.377	3.156852296	3.150507828	0.1462543574
-10	0.543	3.221463968	3.212334456	0.2171611629
-7.5	0.693	0.273583267	0.2663182107	0.2931996757
-5	0.807	3.314005227	3.307781621	0.3388087874
-2.5	0.852	3.384401429	3.376998772	0.3727869074
0	1	3.405348873	3.397583797	0.3912216783
2.5	0.852	3.387717067	3.377432991	0.3727213215
5	0.807	3.314401833	3.310231437	0.3232324048
7.5	0.693	3.274585031	3.266510493	0.2914618817
10	0.543	3.219533271	3.21471119165	0.2169361
12.5	0.377	3.152163862	3.150324208	0.1461857766
15	0.237	3.099729038	3.096283293	0.0869312166
17.5	0.138	3.065349863	3.06863768	0.0867170347
20	0.09	3.657257275	3.65770788	0.0377287809
Weighting	8.79%	3.405732568	3.398428268	0.3926229713



Stage 3 evaluated the aerodynamic performance of an extended ExAero configuration combining the Gladius ALTA raised cockpit, a one-size-smaller frame, and the MAG Aero Bottle system.

With the same rider position maintained, the complete ExAero RDC configuration — Gladius ALTA cockpit, two MAG aero bottles, and a one-size-smaller frame — reduced weighted CdA by 0.00992 m^2 compared with the Spear RDC using conventional bottles, equivalent to approximately 11.63 W at 45 km/h.

With the more extreme low-drag setup using a single down-tube MAG aero bottle, ExAero RDC reduced weighted CdA by 0.01213 m^2 relative to the Spear RDC with two conventional bottles, equivalent to approximately 14.21 W at 45 km/h.

For riders who can accommodate this setup and prioritize aerodynamic efficiency, this configuration provides a clear performance advantage in racing conditions.

3 Torsional Stiffness

Rather than minimizing projected area at the expense of structure, ExAero retains sufficient cross-sectional area in key load-bearing regions while meeting its aerodynamic targets. This provides a strong structural basis for improving stiffness.

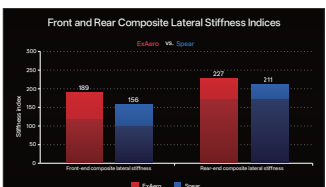

Through optimized structural dimensions and carbon-fiber layup, ExAero achieves a clear increase in stiffness compared with Spear.

The front-end composite lateral stiffness index increases from 156 to 189, a gain of approximately 21.2%, providing a stiffer platform for steering and handling. The rear-end index increases from 211 to 227, a gain of approximately 7.6%, improving pedaling stiffness and response.

4 System Weight

Weight Comparison

ExAero vs. Spear

Unit: g

Category	Component	ExAero	Spear	Difference
Core Parts	Frame	820.0	685.0	+135.0
	Fork	395.0	410.0	-15.0
	Handlebar	308.0	310.0	-2.0
	Core parts Subtotal	1,523.0	1,405.0	+118.0
Components	Derailleur Hanger	22.0	12.5	+9.5
	Seatpost Wedge and Bolts	8.8	17.9	-9.1
	Seatpost Sealing Plug and Bottom-Bracket Cover	6.8	7.0	-0.2
	Headset Spacer Set	52.5	48.0	+4.5
	Stem Cover	11.0	9.0	+2.0
	Computer Mount	29.0	28.9	+0.1
	Front Thru-Axle	23.5	22.3	+1.2
	Rear Thru-Axle	33.8	29.5	+4.3
	Fork Steerer Nut	5.5	6.0	+1.5
	Chainstay Protector	1.7	2.2	-0.5
	Components Subtotal	194.6	181.3	+13.3
	Total of Differing Components	1,717.6	1,586.3	+131.3

For the core parts, the listed weights are net component weights excluding paint and accessories.

In the development of ExAero, weight was treated as a constrained design variable rather than a metric to be minimized in isolation. Additional mass was accepted only where it provided a clear structural or aerodynamic benefit.

On an equivalent-specification basis, the listed ExAero and Spear components weigh 1,717.6 g and 1,586.3 g respectively, a difference of 131.3 g, or approximately 8.3%. The frame accounts for a 135.0 g increase, while the fork and handlebar together save 17.0 g, resulting in a net increase of 118.0 g in the core structure. The remaining supporting and integration components add a net 13.3 g.

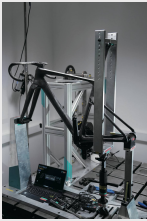

5 Geometry

Geometry

The responsiveness and handling of a road bike are largely determined by its geometry and overall stiffness. Geometry can be considered in two areas: fit geometry, which defines the rider's position and cockpit dimensions, and handling geometry, which governs the bike's dynamic behavior.

For rider fit, the aim is to balance comfort with an aggressive race position. Previous SEKA models placed greater emphasis on a position suited to sustained, consistent riding. With the addition of the Gladius ALTA integrated cockpit, ExAero can use a frame geometry closer to current race-oriented fit requirements while retaining adjustment range. Compared with Spear, ExAero has slightly more reach and less stack for a more aggressive position. Riders who require a higher stack can use the ALTA cockpit to increase effective stack by 25 mm without adding spacers.

For sizing, ExAero replaces the two separate Racing-geometry sizes used previously with a more closely spaced and linear seven-size range, providing finer fit options across different rider heights and riding positions.

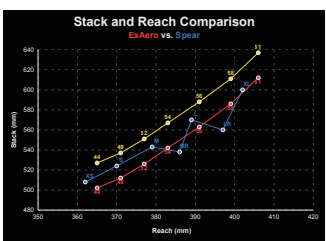

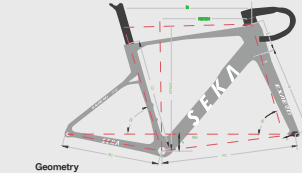

Geometry

SIZE	STACK	REACH	TRAIL	C1	RC	H	FC	WB	L	N	Q1	Q2	F	G	STANDOVER (mm)
44	502	360	70.6	440	400	75	571	967	89	494.8	70.6	75.6	47	369.7	716
49	512	371	64.8	449	400	75	573	969	106	503.4	71.4	75.6	47	369.7	725
52	526	377	58.5	460	400	74	574.5	971	118	507.9	72.4	74	47	369.7	739
54	542	383	58	480	400	73	577	974	133.7	518.4	73	74	44	369.7	757
56	563	391	57	500	400	73	586.5	986	154.4	569	73.2	73.6	44	369.7	776
58	584	396	56.6	520	400	73	602	998	177.7	629.8	73.4	73.6	44	369.7	797
61	612	406	54	544	400	72	615	1012	205	683.1	73.6	73	44	369.7	822

In terms of handling, ExAero retains the quick, direct race-oriented character of Spear, with minor adjustments to the fork geometry on smaller sizes to maintain consistent steering feedback and handling across the size range. The chainstay length has also been reduced from 410 mm to 408 mm, together with an increase in BB drop. The more compact rear-end geometry and slightly shorter wheelbase give ExAero a more immediate response under acceleration on flat roads and improve steering transitions through consecutive high-speed corners.


EXNERO
P ZERO
SCORPE
ARTECH
EXNERO

References

Peer-Reviewed Technical Literature

Barry, N. (2018). A new method for analysing the effect of environmental wind on real world aerodynamic performance in cycling. Proceedings, 2(6), Article 211. https://doi.org/10.3390/proceedings2060211

Crouch, T. N., Burton, D., Brown, N. A. T., Thompson, M. C., & Sheridan, J. (2014). Flow topology in the wake of a cyclist and its effect on aerodynamic drag. Journal of Fluid Mechanics, 748, 5–35. https://doi.org/10.1017/jfm.2013.678

Crouch, T. N., Burton, D., Thompson, M. C., Brown, N. A. T., & Sheridan, J. (2016). Dynamic leg-motion and its effect on the aerodynamic performance of cyclists. Journal of Fluids and Structures, 65, 121–137. https://doi.org/10.1016/j.jfluidstructs.2016.05.007

Crouch, T. N., Burton, D., LaBry, Z. A., & Blair, K. B. (2017). Riding against the wind: A review of competition cycling aerodynamics. Sports Engineering, 20(2), 81–110. https://doi.org/10.1007/s12283-017-0234-1

Griffith, M. D., Crouch, T., Thompson, M. C., Burton, D. M., Sheridan, J., & Brown, N. A. T. (2014). Computational fluid dynamics study of the effect of leg position on cyclist aerodynamic drag. Journal of Fluids Engineering, 136(10), Article 101105. https://doi.org/10.1115/1.4027428

Martin, J. C., Douglas, M. L., Cobb, J. E., McFadden, K. L., & Coggan, A. R. (1998). Validation of a mathematical model for road cycling power. Journal of Applied Biomechanics, 14(3), 276–291. https://doi.org/10.1123/jab.14.3.276

Glossary A

Aerodynamic Drag

The force that resists the motion of the rider and bicycle through the air.

Aerodynamic Power

The power required to overcome aerodynamic drag at a given speed.

Baseline

The reference configuration used to calculate and compare differences between test setups.

CdA

The product of drag coefficient and frontal projected area, used to represent the aerodynamic drag area of a given configuration.

CFD (Computational Fluid Dynamics)

Numerical simulation of the airflow around the bicycle and its components.

Cd (Drag Coefficient)

A dimensionless parameter describing aerodynamic drag relative to area and dynamic pressure.

ΔCdA

The difference in CdA between two configurations being compared.

Yaw Angle

The angle between the bicycle's direction of travel and the effective airflow direction.

Frontal Projected Area

The two-dimensional silhouette area of the bicycle or bicycle–rider system on a plane perpendicular to the airflow.

Yaw-Weighted CdA

The weighted mean CdA calculated from the probability of different yaw angles under the selected riding conditions.

Measurement Repeatability

The degree to which repeated measurements under the same conditions produce consistent results.

Test Configuration

The complete setup used for a test, including the bicycle, components, rider position, and environmental conditions.

System Weight

The total mass of the frame, fork, cockpit system, and related integration components defined for the comparison.

Appendix A

Cycling Power Calculation Equations

Aerodynamic drag is calculated as:

$$F_{\text{Aero}} = \frac{1}{2}\rho C_d A V^2$$

The power required to overcome aerodynamic drag is:

$$P_{\text{Aero}} = F_{\text{Aero}} V = \frac{1}{2}\rho C_d A V^3$$

The difference in aerodynamic power between two configurations is:

$$\Delta P_{\text{Aero}} = \frac{1}{2}\rho \Delta(C_d A) V^3$$

Rolling-resistance power is:

$$P_{\text{RR}} = C_{rr} m g V \cos\theta$$

The power required to overcome an increase in gravitational potential energy is:

$$P_{\text{Gradient}} = mgV \sin\theta$$

In the constant-speed model, the main power requirements are combined as:

$$P_{\text{Total}} = P_{\text{Aero}} + P_{\text{RR}} + P_{\text{Gradient}}$$

where:

- F_{Aero} is aerodynamic drag force
- ρ is air density
- $C_d A$ is drag area
- V represents relative airspeed in the aerodynamic equations and ground speed in the rolling-resistance and gradient equations. The calculations in this report assume no wind, so the two speeds are equal.

Appendix B

Aerodynamic–Weight Crossover Analysis

This appendix describes the calculation model and derivation used for the aerodynamic–weight crossover analysis presented in the main text.

The analysis compares two design benefits:

- A 3 W reduction in aerodynamic power demand at 45 km/h.
- A 120 g reduction in system mass.

To remain consistent with the main analysis, the calculations use a simplified steady-state cycling power model.

B.1 Basic Power Model

At constant speed, the primary power demand is made up of aerodynamic drag, rolling resistance, and gradient resistance:

$$P = \frac{1}{2}\rho C_d A\left(\frac{v}{3.6}\right)^3 + gm\left(C_{rr} + \frac{G}{100}\right)\left(\frac{v}{3.6}\right)$$

In this simplified model, road gradient is represented directly by G / 100, consistent with the steady-state road-riding conditions considered in the main analysis.

B.2 Weight Benefit

The difference in system mass is defined as: $\Delta m = 0.12\,\mathrm{kg}$

At a given speed v and gradient G, the corresponding power difference associated with a 120 g reduction in system mass is:

$$\Delta P_{\mathrm{Mass}} = g \cdot \Delta m \cdot \left(C_{rr} + \frac{G}{100}\right) \cdot \left(\frac{v}{3.6}\right)$$

Unlike the aerodynamic power saving, the benefit of lower mass increases with gradient and varies approximately linearly with speed.

B.3 Aerodynamic Benefit

At 45 km/h, 3 W corresponds to: $\Delta\ C_dA = 0.00256m^2$

Since aerodynamic power scales with the cube of speed, the corresponding power saving at any speed v is:

$$\Delta P_{\text{Aero}}(v) = 3\left(\frac{v}{45}\right)^3$$

This relationship follows from the basic equations below:

Basic Physical Relations:

$$P = \underset{\text{Power (W)}}{\frac{W}{t}} \quad \underset{\text{Work (J)}}{W} = Fs \quad \underset{\text{Speed}}{\mathcal{U}} = \underset{\text{Distance (m)}}{\frac{S}{t}} \quad \underset{\text{Time (s)}}{t}$$

$$P = \frac{Fs}{t} \qquad P = Fv$$

Aerodynamic drag equation: $F_D = \frac{1}{2}\rho C_d A v^2$

$$P = \frac{1}{2}\rho C_d A v^3$$

Given: $\Delta P(45) = 3\,\text{W}$

Therefore: $\frac{\Delta P(v)}{\Delta P(45)} = \left(\frac{v}{45}\right)^3$

$\Delta P \propto v^3$ (Change in power Proportional to Speed cubed)

Thus: $\Delta P_{\text{Aero}}(v) = 3\left(\frac{v}{45}\right)^3$

B.4 Crossover Point Definition

The aerodynamic–weight crossover point is defined as the condition where:

$$\Delta P_{\text{Aero}}(v) = \Delta P_{\text{Mass}}$$

$$3 \times \left(\frac{v}{45}\right)^3 = g \times 0.12 \times \left(Crr + \frac{G}{100}\right)\left(\frac{v}{3.6}\right)$$

B.5 Derivation of Crossover Speed

Using the total power equation for the aerodynamic system together with the crossover condition defined in Section B.4:

$$P = \frac{1}{2}\rho C_d A_{aero}\left(\frac{v}{3.6}\right)^3 + gm_{aero}\left(Crr + \frac{G}{100}\right)\left(\frac{v}{3.6}\right)$$

the crossover speed v^* can be expressed as:

$$v^* = 3.6 \times \sqrt[3]{\frac{2P}{\rho\left[C_d A_{aero} + \left(\frac{m_{system}}{\Delta m}\right)\Delta C_d A\right]}}$$

This shows that, with the other parameters fixed, rider power determines the corresponding crossover speed.

B.6 Derivation of Crossover Gradient

Once the crossover speed v* has been determined, substituting it back into the crossover condition gives the corresponding crossover gradient:

$$G = 100 \times \left\{\frac{3 \times (v^*/45)^3}{g \times \Delta m \times (v^*/3.6)} - Crr\right\}$$

This gives the crossover gradient and crossover speed corresponding to each rider power output.

B.7 Crossover Results

Using the following fixed parameters:

Parameter	Value
Reference CdA	3.3398 m²
Aerodynamic Advantage	3.0 W at 45 km/h
Equivalent ΔCdA	0.002556 m²
System Mass Difference	0.1200 kg
Reference System Mass	85.0 kg
Air Density	1.20 kg/m³
Crr	0.003

This gives:

Rider Power	Crossover Gradient	Crossover Speed
250 W	4.1%	20.8 km/h
300 W	4.6%	22.1km/h
350 W	5.2%	23.3km/h
400 W	5.7%	24.4km/h
450 W	6.2%	25.3km/h

B.8 Calculation of Non-Crossover Points

Aero-optimized system:

$$P = \frac{1}{2}\rho C_d A_{\text{aero}} \left(\frac{v_{\text{aero}}}{3.6}\right)^3 + g m_{\text{aero}} \left(Crr + \frac{G}{100}\right) \left(\frac{v_{\text{aero}}}{3.6}\right)$$

Lightweight system:

$$P = \frac{1}{2}\rho C_d A_{\text{ligt}} \left(\frac{v_{\text{ligt}}}{3.6}\right)^3 + g m_{\text{ligt}} \left(Crr + \frac{G}{100}\right) \left(\frac{v_{\text{ligt}}}{3.6}\right)$$

After solving for the speed of each system, the results are converted to time per kilometer (s/km) and compared.

By varying the road gradient G and repeating the calculation, the complete curves for different rider power outputs can be generated.

B.9 Model Scope and Limitations

This analysis is intended to describe the relative relationship between a fixed aerodynamic difference and a fixed mass difference under steady-state riding conditions.
The model assumes:

- Constant rider power
- Constant road gradient
- Steady-state riding speed
- Unchanged rider position
- Constant air density and rolling resistance coefficient
- No acceleration, drivetrain-efficiency differences, changes in environmental wind, or variations in pacing during actual racing

The model is therefore intended to describe the performance boundary between aerodynamic and weight benefits, rather than to predict total riding time in an actual race.

Appendix C

Data Scope and Limitations

The data presented in this report describe the test configurations and analytical conditions defined for this project. All results should be interpreted in the context of the stated test methods, reference conditions, and component configurations.

Aerodynamic Data

CFD results are numerical approximations of airflow and depend on the geometry model, mesh, turbulence model, and boundary conditions used.

Wind-tunnel results include measurement uncertainty, variation in rider position, and normal run-to-run variation. Relative comparisons within the same test session are more reliable than comparisons of absolute values across different dates or test setups.

Power differences calculated from CdA apply only to the stated airspeed and air density.

Structural Data

Stiffness results apply only to the defined fixtures, loading directions, and displacement measurement locations. Results obtained using different test methods may not be directly comparable.

The overall stiffness values reported here are integrated comparison indices rather than universal stiffness units.

Carbon-fiber structures may show limited production variation due to layup tolerances, material batches, curing conditions, and surface finishing.

Geometry and Handling

Geometry data represent nominal production-design values. Tire size, wheel dimensions, cockpit configuration, and spacer setup may affect the final position of the complete bike.

Handling descriptions reflect the intended effect of the geometry changes. Rider perception will also depend on body dimensions, riding position, speed, tire choice, and riding technique.

Weight Data

Component weights may vary slightly between production samples. When comparing published weights, the specifications for paint, hardware, steerer length, and accessory configuration should be clearly defined.

Data Presentation and Rounding

Some values have been rounded for clarity. Small differences between displayed totals and independently recalculated values may result from rounding of the underlying measurements.

Interpretation of Results

Unless otherwise stated, all comparisons in this report are based on the defined test configurations and should not be treated as universal values for all riders, environments, or component combinations.

This appendix is intended to define the scope of the data, not to diminish the results presented in the report. Within the stated methods and conditions, the data remain a valid basis for comparison.

SEKA



EXNERN

www.sekabikes.com